

# Matching the Clinical Reality: Accurate OCT-Based Diagnosis From Few Labels

Valentyn Melnychuk<sup>a,b</sup>, Evgeniy Faerman<sup>b</sup>, Ilja Manakov<sup>b</sup> and Thomas Seidl<sup>b</sup>

<sup>a</sup>Fraunhofer Institute for Integrated Circuits IIS, Erlangen, Germany

<sup>b</sup>Ludwig Maximilian University of Munich, Germany

## Abstract

Unlabeled data is often abundant in the clinic, making machine learning methods based on semi-supervised learning a good match for this setting. Despite this, they are currently receiving relatively little attention in medical image analysis literature. Instead, most practitioners and researchers focus on supervised or transfer learning approaches. The recently proposed MixMatch and FixMatch algorithms have demonstrated promising results in extracting useful representations while requiring very few labels. Motivated by these recent successes, we apply MixMatch and FixMatch in an ophthalmological diagnostic setting and investigate how they fare against standard transfer learning. We find that both algorithms outperform the transfer learning baseline on all fractions of labelled data. Furthermore, our experiments show that exponential moving average (EMA) of model parameters, which is a component of both algorithms, is not needed for our classification problem, as disabling it leaves the outcome unchanged. Our code is available online: <https://github.com/Valentyn1997/oct-diagn-semi-supervised>.

## Keywords

Semi-supervised image classification, Transfer learning, Optical Coherence Tomography

## 1. Introduction

In recent years deep learning techniques have taken the field of AI by storm. Virtually all state-of-the-art systems in computer vision (CV) rely on some form of deep learning. This paradigm shift has sparked the imagination of many practitioners and researchers in the medical image analysis domain. Computer-aided diagnosis appeared to be next-in-line to benefit from the advancements made in CV, as the amount of data in clinical diagnostics is increasing rapidly. The research community has proposed a plethora of new algorithms and systems for the automated diagnosis of a wide range of diseases. However, clinical adoption has been slow. One crucial reason is that supervised learning, which forms the basis for the vast majority of deep learning approaches, is ill-suited to the medical domain.

This mismatch is two-fold. For one, the labelled data needed for supervised learning is prohibitively costly to generate for medical applications. With a shortage of medical practitioners, diverting medical experts' time and energy to labelling efforts becomes exceedingly expensive. More fine-grained problem formulations (e.g. single-label vs. multi-label, volume level vs. slice level

annotation, etc.) result in exponentially more labelling expenses. Additionally, most clinics lack the tools to label vast amounts of data. Secondly, and perhaps more fundamentally, there is an epistemic problem in generating accurate labels. For any given diagnostic problem, the inter-expert agreement is well below 100%. This discrepancy stems from the fact that medicine is complex and does not always fit neatly into a classification formulation. Additionally, each expert comes with his or her own set of experiences and knowledge.

Instead of solely relying on supervised learning, semi-supervised learning (SSL) should discover the bulk of the knowledge required for solving a diagnostic task on its own, with labels only serving as additional guidance. The idea of SSL is to train a machine learning algorithm on vast amounts of unlabeled data and a small set of labelled samples. SSL is a much better match for the clinical setting, as unlabeled data is often abundant since it is acquired as part of the clinical routine.

In this work, we apply two recently proposed SSL methods, MixMatch [1] and FixMatch [2], to a diagnostic problem in ophthalmology. We test which performs better in classifying optical coherence tomography (OCT) b-scans into four classes (one healthy and three pathological) at different fractions of labelled data. We compare the two SSL methods to a baseline transfer learning approach, similar to [3]. After going over related work in the next section, we explain the basis for our experiments in Section 3, covering MixMatch, FixMatch and the transfer learning baseline. In Section 4 we describe the dataset and present the results of our

*Proceedings of the CIKM 2020 Workshops, October 19-20, 2020, Galway, Ireland*

✉ v.melnichuk@campus.lmu.de (V. Melnychuk);

faerman@dbs.ifi.lmu.de (E. Faerman); ilja.manakov@gmx.de (I. Manakov); seidl@dbs.ifi.lmu.de (T. Seidl)

🆔 0000-0002-2401-6803 (V. Melnychuk); 0000-0002-4861-1412 (T. Seidl)



© 2020 Copyright for this paper by its authors. Use permitted under Creative Commons License Attribution 4.0 International (CC BY 4.0).

CEUR Workshop Proceedings (CEUR-WS.org)

investigation. We conclude with Section 5 by summarizing our findings and discussing how they apply to the clinical setting.

## 2. Related work

**Semi-supervised learning.** State-of-the-art methods for image classification concentrate on finding the right combination of SSL paradigms. One of the early approaches – Mean-Teacher [4] – uses exponential moving average (EMA) of model parameters. Virtual Adversarial Training (VAT) [5], tries to find a minimal perturbation and fit a robust model against it. MixMatch [1] and ReMix [6] encompass mixing and overlaying labelled and unlabelled images to obtain consistent predictions. Unsupervised Data Augmentation (UDA) [7] uses strongly augmented images to force consistency among unlabeled images. ReMixMatch [8] uses so-called “augmentation anchoring”, i.e. strong and weak augmentations, to enforce consistency. Inspired by UDA and ReMixMatch, the authors of FixMatch [2] significantly simplify SSL by relying only on augmentations and pseudo-labelling with a confidence threshold. We provide a broader overview of applied SSL methods in Section 3.2.

Surprisingly, there exists only a little amount of literature on SSL applied to ophthalmological data. [9] and [10] utilize SSL for OCT segmentation. In the domain of automated diagnosis, [11] employ an autoencoder with an additional classification module on the latent code in the detection of retinopathy from colour fundus images. [12] tackle the same problem by extending the GAN framework [13] to one “fake” and six “real” classes, i.e. the labeled classes. Recent works [14] and [15] apply the same principle to the classification of OCT b-scans. Most recently, [16] applied SSL methods to glaucoma detection by imputing missing visual field (VF) measurements through nearest-neighbour identification in the latent space of a pre-trained classification CNN. Afterwards, [16] train a multi-task network jointly on glaucoma classification and VF measurement prediction. To the best of our knowledge, we are the first to apply consistency regularization based SSL techniques (see Section 3) to the problem of automated diagnosis in ophthalmology.

**Transfer learning.** Among numerous approaches existing in the deep transfer learning [17], we choose the fine-tuning or network-based transfer learning to be the most promising. [18, 19] proposed to use ImageNet [20] pre-trained CNN as the initialization for different visual recognition tasks with the limited amount

of labels. Yosinski et al. [21] discovered how unfreezing different parts of the network while fine-tuning affects the target performance.

## 3. Approach

Transfer learning and semi-supervised learning are two main approaches for predictive modelling when dealing with data with few labels. Transfer learning approaches reuse knowledge from previously learned tasks. On the other hand, the SSL approaches allow learning with small labelled datasets by utilizing unlabeled data from the same distribution in the learning process. In the following, we first discuss our transfer learning baseline and afterwards describe the SSL approaches we have chosen for this study.

### 3.1. Transfer Learning

When applying transfer learning techniques, the user has to choose how to adapt the model from the auxiliary to the primary task. In our experiments, we use a network, which was pre-trained on ImageNet [20]. For adapting the model to OCT classification we try two common approaches. In the *feature extraction* approach, we freeze all parameters except for the final fully connected layer, analogous to [3]. Alternatively, we use the pre-trained network as initialization and allow all parameters to change. We refer to this as *fine-tuning* hereafter.

### 3.2. Semi-supervised Learning

In our study we compare two of recent state-of-the-art algorithms for SSL *MixMatch* [1] and *FixMatch* [2]. Both algorithms combine several pre-existing techniques from SSL. In this chapter, we review the main ideas and compare their utilization in both algorithms. We refer the reader to Appendix A for the detailed algorithm descriptions.

**Data Augmentation.** Data Augmentation is a regularization technique which is often used in supervised learning. The goal is that the model’s prediction is not affected by the certain transformation of data instances. Therefore additional training data is added to the dataset by applying various perturbations to the data while keeping original labels. Most of the data augmentations are domain-specific and require domain knowledge.

*MixMatch* uses random flip-and-shift augmentations (horizontal flips and random crops) for both labelled and unlabeled data.

*FixMatch* distinguishes between *weak* and *strong* data augmentations. Flip-and-shift augmentations are considered as weak augmentations, whereas affine transformations and color-jittering are examples of strong augmentations (originally – 14 different transformations from RandAugment [22]).

**Pseudo-Labeling.** Pseudo-Labeling or self-training loss [23] is the process of using the trained model to obtain labels for unlabeled instances. The predicted labels are used to guide the further learning process, e.g. by using generated labels as new targets.

*MixMatch* applies different augmentations for an unlabeled instance and computes the class distribution for each augmentation. Therefore, instead of *hard* one hot label *MixMatch* defines a probability distribution as the target. To sharpen the distribution and to reduce its entropy, the temperature of distribution is adjusted [24].

*FixMatch* uses a “classic” version of pseudo-labelling with hard labels and fixed confidence. The class probability distribution is taken from model outputs after a weak augmentation. If the probability of the most probable class exceeds a predefined threshold the label is assigned to a strongly augmented version of the same instance and used in the loss calculation.

**Consistency Regularization.** Consistency regularization [25] imposes the constraint that the model should make similar predictions for the same instance under different data augmentations. Both *MixMatch* and *FixMatch* apply data augmentation on labelled and unlabeled data and enforce similar prediction for the same instance under different augmentations. For the unlabeled instances, the pseudo-label is used as a target. *FixMatch* uses soft augmentations to compute pseudo-labels for hard augmentations of the same training sample.

**EMA decay.** Another popular consistency requirement in SSL is an exponential moving average (EMA) of model parameters over time to smooth the behaviour when the model changes its decisions rapidly. The EMA is the basis of Mean Teacher algorithm [4], which maintains two models. The *teacher* model stores an exponential moving average of *student*’s parameters and is used to make the predictions to compute the pseudo-labels. Therefore pseudo-labels computed by

the teacher can be considered as a weighted combination of decisions of previous models. The *student* model makes the predictions for the training data and is updated based on the training loss. Both *MixMatch* and *FixMatch* employ EMA decay while inference. Note, that keeping a second model in memory and updating its parameters results in higher memory requirements and computation costs.

**MixUp.** MixUp [26] is another regularization technique to avoid overfitting. MixUp linearly combines training instance pairs and their prediction targets. Therefore it tries to impose linear behaviour between training samples. *MixMatch* does not differentiate between *pseudo* targets predicted for the unlabeled instances and *ground truth* labels and mixes all possible target pairs. Therefore a resulting instance used in training may be a combination of two pseudo targets, two ground truth labels or of pseudo-target with ground truth label.

## 4. Experiments

Our work follows the principles of the fair SSL evaluation framework, defined by [27]. The authors highlight the importance of using the same classifying model structure for comparison. The evaluation is also meaningful for the real use-case if SSL methods are compared with well-fine-tuned transfer learning and fully supervised models.

For the evaluation we use the **UCSD dataset** published by Kermany et al. [3]. It contains 84,495 optical coherence tomography (OCT) b-scans pertaining to four categories; “normal”, “drusenoid” (DRUSEN), “choroidal neovascularization” (CNV) and “diabetic macular edema” (DME). The images vary in size, where the median image has a size of 496×512 pixels. The height of the images ranges between 496 and 512 and the width between 384 and 1536. The dataset is also obtainable through Kaggle<sup>1</sup>. For better comparability, we use the same train/validation/test split as in the Kaggle challenge. There are several images for each patient in the dataset and splits are done patient-wise, there are no images of the same patients in different splits. Test and validation are balanced, there are 8 and 242 images per class respectively (see Fig. 1). In our experiments, we vary the number of labelled data, which we sample randomly from the training subset. We sample the same number of labelled training instances from each class. For SSL approaches the rest of the train set is used as unlabeled data.

<sup>1</sup><https://www.kaggle.com/paultimothymooney/kermany2018>.

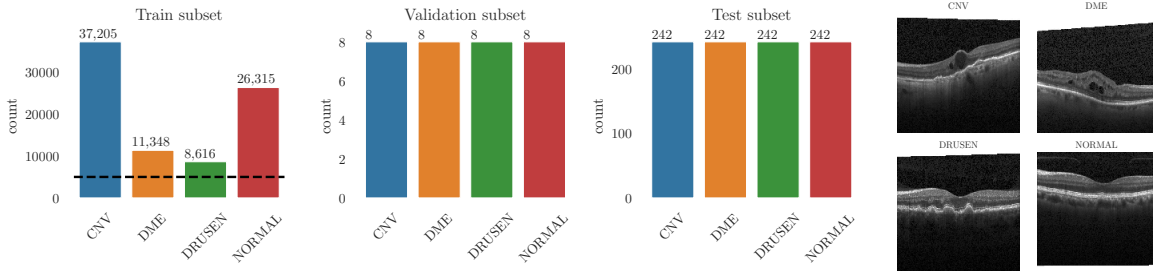


**Figure 1.:** Histogramms of image labels and random image for each class. Horizontal dashed line on train subset subplot denotes labelled-unlabelled split with  $n_l = 20,000$  (upper part corresponds to unlabelled subset). The images on the right depict a sample from each class.

We compare the performance of transfer learning and SSL models using the same **Wide ResNet-50-2** [28] backbone. Since the images are monochrome we duplicate the channel three times for RGB channels.

For each model, we perform hyperparameter search, described in Appendix B.1 and B.2. For all experiments, we report the model performance on test data in the epoch with the lowest validation loss.

#### 4.1. Comparison of transfer learning and SSL approaches

First, in Table 1 we compare the performance of our backbone model trained with all labelled instances to the results reported previously in the literature for the same UCSD dataset. As we can see, the backbone model achieves almost perfect performance when trained with enough labels.

Next, in Fig. 2b we compare two transfer learning approaches. Note, that the hyperparameter search was done for each number of labels for each approach. We discover that, contrary to our expectations, the fine-tuning variant outperforms feature extraction approach in all label settings. We believe that a thorough selection of hyperparameters with representative validation set reduces the risk of overfitting. Furthermore, since the original models are trained on the dataset with RGB channels, we believe that the model can better adapt to the monochrome setting when all model weights are allowed to be changed.

In the Fig. 2a we present the results of both SSL algorithms and compare them with the best performing transfer learning setting. We find that the SSL approaches outperform transfer learning on all fractions of labelled data. The gap between SSL and transfer learning widens significantly for smaller fractions of labelled data. With only 10 labelled representatives per class, the FixMatch achieves an accuracy of over 86%,

Method	$n_l$	Accuracy	Notes
Kermany et al. [3]	All	96.6%	Original paper
Alqudah [29]	All	97.1%	Extended UCSD with 5 classes
Wu et al. [30]	All	97.5%	
Chetoui et al. [31]	All	98.46%	
Tsuji et al. [32]	All	99.6%	
<b>WideResNet-50-2 (our backbone)</b>	All	<b>99.69%</b>	With EMA decay ( $\beta_{EMA} = 0.999$ )
He et al. [14]	835	87.25±1.44% *	*Average precision

**Table 1.**

Reported test accuracies for UCSD dataset. Methods have different backbones and thus are not fully comparable with the proposed SLL methods. Nevertheless, our best fully-supervised model outperforms previously reported methods.

while transfer learning reaches only 59%. We also see, that with about 2000-4000 labels all methods achieve almost perfect performance. The *Fix-Match* algorithm also outperforms *Mix-Match* in almost all settings and with only 50 labelled points per class achieves the accuracy of 98.14%. We also observe a small SSL performance drop for 25 labelled images per class – mainly because methods require even more epochs to fit (we employ a heuristical formula for defining the maximum number of epochs based on the number of labels, see Appendix B.2, 3).

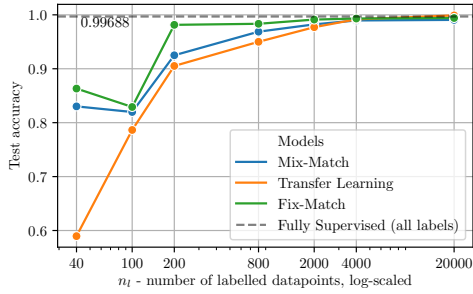
Finally, since practitioners have often to deal with the resource constraints and actual running times are rarely reported in the literature, we report them in Table 2. Note, that all methods are implemented in the same framework and the experiments are done on the same machine with two Tesla V100 Nvidia GPUs. To use the same batch size as recommended in the original publications, we have used both GPUs to train *Fix-Match*. Other models are trained on a single GPU.



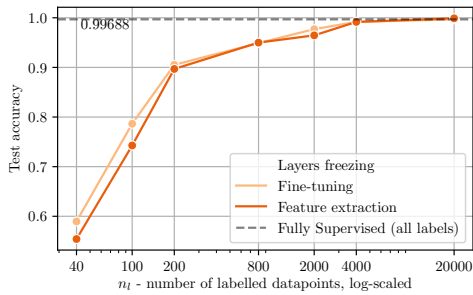
$n_l$	40	100	200	800	2000	4000	20000
Transfer Learning	10m	9m	12m	15m	24m	39m	1h 39m
Mix-Match	1d 16h 5m	9h 12m	6h 13m	2h 30m	2h 37m	2h 24m	2h 26m
FixMatch	5d 9h 36m	1d 19h 4m	1d 40m	9h 58m	10h 40m	9h 50m	7h 51m

**Table 2.**

Training time comparison between the best models of each approach for varying number of labels  $n_l$ . We do not include the time, spent on hyperparameter search and report only the training time of single models.



(a) Best models, maximum performance among 4 runs (Semi-supervised) / 8 runs (Transfer learning) per each  $n_l$



(b) Study of layers freezing for Transfer learning, maximum performance among 4 runs per each  $n_l$ .

**Figure 2.:** Test accuracies for SSL and Transfer learning models for varying number of labels  $n_l$ . Fully-supervised baseline with all labels uses EMA decay ( $\beta_{EMA} = 0.999$ ).

## 4.2. EMA decay

The *EMA* is inherent part of *Fix-Match* algorithm and is also optionally recommended for *Mix-Match*. We observe learning curve to be more stable for validation subset for all the models when models are trained using it. However, we assume that with the right chosen validation subset, the variability could be advantageous and one can find a better fit. Usage of *EMA* model causes additional computation and memory costs and as can be seen in Table 3 most of the time models without it perform better.

## 5. Conclusion

In this work, we have demonstrated the efficacy of MixMatch and FixMatch, when applied to an ophthalmological diagnostic problem on OCT data. The two algorithms were able to attain high accuracy, achieving well over 80% on as little as 40 labelled samples (i.e. ten per class). Both algorithms outperformed transfer learning in the few labelled data settings. This study emphasizes the use of SSL methods in the clinical adoption of AI. Although both MixMatch and FixMatch are more computationally expensive than transfer learning, the amount of labelling effort saved by using them is immense. With labelling being one of the biggest factors hindering clinical use of AI methodology, we argue that smarter use of the abundance of unlabeled data already present at the clinic will be a major strategy for overcoming this hurdle.

As part of future work, we propose to also compare SSL approach with the few-shot deep learning.

## References

- [1] D. Berthelot, N. Carlini, I. Goodfellow, N. Papernot, A. Oliver, C. A. Raffel, Mixmatch: A holistic approach to semi-supervised learning, in: Advances in Neural Information Processing Systems, 2019, pp. 5049–5059.
- [2] K. Sohn, D. Berthelot, C.-L. Li, Z. Zhang, N. Carlini, E. D. Cubuk, A. Kurakin, H. Zhang, C. Raffel, Fixmatch: Simplifying semi-supervised learning with consistency and confidence, ArXiv abs/2001.07685 (2020).
- [3] D. S. Kermany, M. Goldbaum, W. Cai, C. C. Valentin, H. Liang, S. L. Baxter, A. McKeown, G. Yang, X. Wu, F. Yan, et al., Identifying medical diagnoses and treatable diseases by image-based deep learning, Cell 172 (2018) 1122–1131.
- [4] A. Tarvainen, H. Valpola, Mean teachers are better role models: Weight-averaged consistency targets improve semi-supervised deep learning results,

	$n_l$		40		100		200		800		2000		4000		20000	
	$\beta_{EMA}$		0.0	0.999	0.0	0.999	0.0	0.999	0.0	0.999	0.0	0.999	0.0	0.999	0.0	0.999
Transfer Learning			58.96	—	78.65	—	90.52	—	95.00	—	97.71	—	98.23	—	99.38	—
Mix-Match			83.02	55.00	75.73	81.98	92.50	88.85	94.69	96.88	98.02	98.23	98.02	98.96	99.06	98.75
FixMatch			<b>86.33</b>	72.66	<b>82.91</b>	75.88	97.07	<b>98.14</b>	<b>98.34</b>	98.05	97.85	<b>99.12</b>	98.34	<b>99.32</b>	98.63	<b>99.41</b>

**Table 3.**

Best test accuracy based on several runs (8 runs with varying learning rate, weight decay and back-bone unfreezing for Transfer Learning, 2 runs with a varying total number of batches for MixMatch and FixMatch) for varying number of labels  $n_l$ . We do not observe any profit of using / not using EMA decay ( $\beta_{EMA}$ ) for all methods, unlike previously reported results.

- in: Advances in neural information processing systems, 2017, pp. 1195–1204.
- [5] T. Miyato, S.-i. Maeda, M. Koyama, S. Ishii, Virtual adversarial training: a regularization method for supervised and semi-supervised learning, *IEEE transactions on pattern analysis and machine intelligence* 41 (2018) 1979–1993.
- [6] V. Nair, J. F. Alonso, T. Beltramelli, Realmix: Towards realistic semi-supervised deep learning algorithms, *arXiv preprint arXiv:1912.08766* (2019).
- [7] Q. Xie, Z. Dai, E. H. Hovy, M.-T. Luong, Q. V. Le, Unsupervised data augmentation for consistency training, *arXiv: Learning* (2019).
- [8] D. Berthelot, N. Carlini, E. D. Cubuk, A. Kurakin, K. Sohn, H. Zhang, C. Raffel, Remixmatch: Semi-supervised learning with distribution alignment and augmentation anchoring, *arXiv preprint arXiv:1911.09785* (2019).
- [9] X. Liu, J. Cao, T. Fu, Z. Pan, W. Hu, K. Zhang, J. Liu, Semi-supervised automatic segmentation of layer and fluid region in retinal optical coherence tomography images using adversarial learning, *IEEE Access* 7 (2018) 3046–3061.
- [10] S. Sedai, B. Antony, R. Rai, K. Jones, H. Ishikawa, J. Schuman, W. Gadi, R. Garnavi, Uncertainty guided semi-supervised segmentation of retinal layers in oct images, in: *International Conference on Medical Image Computing and Computer-Assisted Intervention*, 2019, pp. 282–290.
- [11] S. Liu, J. Xin, J. Wu, P. Shi, Semi-supervised adversarial learning for diabetic retinopathy screening, in: *International Workshop on Ophthalmic Medical Image Analysis*, 2019, pp. 60–68.
- [12] Y. Xie, Q. Wan, G. Chen, Y. Xu, B. Lei, Retinopathy diagnosis using semi-supervised multi-channel generative adversarial network, in: *International Workshop on Ophthalmic Medical Image Analysis*, Springer, 2019, pp. 182–190.
- [13] I. Goodfellow, J. Pouget-Abadie, M. Mirza, B. Xu, D. Warde-Farley, S. Ozair, A. Courville, Y. Bengio, Generative adversarial nets, in: *Advances in neural information processing systems*, 2014, pp. 2672–2680.
- [14] X. He, L. Fang, H. Rabbani, X. Chen, Z. Liu, Retinal optical coherence tomography image classification with label smoothing generative adversarial network, *Neurocomputing* (2020).
- [15] V. Das, S. Dandapat, P. K. Bora, A data-efficient approach for automated classification of oct images using generative adversarial network, *IEEE Sensors Letters* 4 (2020) 1–4.
- [16] X. Wang, H. Chen, A. R. Ran, L. Luo, P. P. Chan, C. C. Tham, R. T. Chang, S. S. Mannil, C. Y. Cheung, P. A. Heng, Towards multi-center glaucoma OCT image screening with semi-supervised joint structure and function multi-task learning, *Medical Image Analysis* 63 (2020). doi:10.1016/j.media.2020.101695.
- [17] C. Tan, F. Sun, T. Kong, W. Zhang, C. Yang, C. Liu, A survey on deep transfer learning, in: *International conference on artificial neural networks*, Springer, 2018, pp. 270–279.
- [18] M. Oquab, L. Bottou, I. Laptev, J. Sivic, Learning and transferring mid-level image representations using convolutional neural networks, in: *Proceedings of the IEEE conference on computer vision and pattern recognition*, 2014, pp. 1717–1724.
- [19] J. Donahue, Y. Jia, O. Vinyals, J. Hoffman, N. Zhang, E. Tzeng, T. Darrell, Decaf: A deep convolutional activation feature for generic visual recognition, in: *International conference on machine learning*, 2014, pp. 647–655.
- [20] J. Deng, W. Dong, R. Socher, L.-J. Li, K. Li, L. Fei-Fei, ImageNet: A Large-Scale Hierarchical Image Database, in: *CVPR09*, 2009.
- [21] J. Yosinski, J. Clune, Y. Bengio, H. Lipson, How transferable are features in deep neural networks?, in: *Advances in neural information processing systems*, 2014, pp. 3320–3328.
- [22] E. D. Cubuk, B. Zoph, J. Shlens, Q. V. Le, Randaugment: Practical automated data augmentation with a reduced search space, *arXiv: Com-*

- puter Vision and Pattern Recognition (2019).
- [23] D.-H. Lee, Pseudo-label: The simple and efficient semi-supervised learning method for deep neural networks, in: Workshop on challenges in representation learning, ICML, volume 3, 2013.
  - [24] G. Hinton, O. Vinyals, J. Dean, Distilling the knowledge in a neural network, arXiv preprint arXiv:1503.02531 (2015).
  - [25] M. Sajjadi, M. Javanmardi, T. Tasdizen, Regularization with stochastic transformations and perturbations for deep semi-supervised learning, in: Advances in neural information processing systems, 2016, pp. 1163–1171.
  - [26] H. Zhang, M. Cisse, Y. N. Dauphin, D. Lopez-Paz, mixup: Beyond empirical risk minimization, arXiv preprint arXiv:1710.09412 (2017).
  - [27] A. Oliver, A. Odena, C. A. Raffel, E. D. Cubuk, I. Goodfellow, Realistic evaluation of deep semi-supervised learning algorithms, in: Advances in neural information processing systems, 2018, pp. 3235–3246.
  - [28] S. Zagoruyko, N. Komodakis, Wide residual networks, CoRR abs/1605.07146 (2016). URL: <http://arxiv.org/abs/1605.07146>. arXiv:1605.07146.
  - [29] A. M. Alqudah, Aoct-net: a convolutional network automated classification of multiclass retinal diseases using spectral-domain optical coherence tomography images, Medical & biological engineering & computing 58 (2020) 41–53.
  - [30] J. Wu, Y. Zhang, J. Wang, J. Zhao, D. Ding, N. Chen, L. Wang, X. Chen, C. Jiang, X. Zou, et al., Attennet: Deep attention based retinal disease classification in oct images, in: International Conference on Multimedia Modeling, Springer, 2020, pp. 565–576.
  - [31] M. Chetoui, M. A. Akhloufi, Deep retinal diseases detection and explainability using oct images, in: International Conference on Image Analysis and Recognition, Springer, 2020, pp. 358–366.
  - [32] T. Tsuji, Y. Hirose, K. Fujimori, T. Hirose, A. Oyama, Y. Saikawa, T. Mimura, K. Shiraishi, T. Kobayashi, A. Mizota, et al., Classification of optical coherence tomography images using a capsule network, BMC ophthalmology 20 (2020) 1–9.
  - [33] D. P. Kingma, J. Ba, Adam: A method for stochastic optimization, arXiv preprint arXiv:1412.6980 (2014).
  - [34] Y. E. Nesterov, A method for solving the convex programming problem with convergence rate  $O(1/k^2)$ , in: Dokl. akad. nauk Sssr, volume 269, 1983, pp. 543–547.

## Acknowledgments

This work has been funded by the German Federal Ministry of Education and Research (BMBF) under Grant No. 01IS18036A and by the Bavarian Ministry for Economic Affairs, Infrastructure, Transport and Technology through the Center for Analytics-Data-Applications (ADA-Center) within the framework of “BAYERN DIGITAL II”. The authors of this work take full responsibilities for its content.

# Appendix

## A. MixMatch & FixMatch – algorithm details

The foundation of both MixMatch and FixMatch is consistency regularization – the idea that augmentations of the same data point should yield the same label. In this way, the model regularizes itself based on its predictions.

Let  $\mathcal{X} = \{(x_b, y_b), b \in (1, \dots, B)\}$  be the batch of labeled examples.  $\alpha(\cdot)$  denotes the set of *weak* augmentations and  $\mathcal{A}(\cdot)$  – *strong* augmentations.  $\hat{y} = f_M(x; \theta)$  is the prediction of backbone classifier, parametrized by  $\theta$ .  $H(\cdot, \cdot)$  denotes categorical cross-entropy and  $\lambda_u$  is unsupervised loss weight.

**MixMatch** employs only weak augmentations  $\alpha(\cdot)$  and MixUp [26]. Let  $\mathcal{U} = \{u_b, b \in (1, \dots, B)\}$  be the unlabeled data batch. The model outputs of  $K$  random weak augmentations  $\alpha(\cdot)$  of the same unlabelled sample are treated as soft pseudo-labels  $q_b$ . These soft pseudo-labels are averaged and sharpened with the temperature  $T$  for each image in  $\mathcal{U}$  to yield a pseudo-label for that image. Then, images from both randomly augmented  $\mathcal{X}$  and  $\mathcal{U}$  are concatenated and shuffled, resulting in set  $\mathcal{W}$ . Afterwards, samples in  $\mathcal{X}$  and  $\mathcal{U}$  are weakly augmented and linearly interpolated with samples from  $\mathcal{W}$ . This results in  $\hat{\mathcal{X}}$  and  $\hat{\mathcal{U}}$  – "mixed-up" versions of augmented labelled and  $K$  unlabelled batches. Coefficients of MixUp are sampled from Beta( $\alpha, \alpha$ ) distribution. The final loss is the sum of categorical cross-entropy for images from  $\hat{\mathcal{X}}$  (supervised part) and Brier score for  $\hat{\mathcal{U}}$  images (unsupervised part):

$$\mathcal{L} = \frac{1}{B} \sum_{(x,y) \in \hat{\mathcal{X}}} H(y, f_M(x; \theta)) + \frac{\lambda_u}{KB} \sum_{(u,q) \in \hat{\mathcal{U}}} \|q - f_M(u; \theta)\|_2^2, \quad (1)$$

MixMatch linearly ramps up  $\lambda_u$  from 0 to its maximum after each batch to reduce the influence of unsupervised part during early stages of training.

**FixMatch** is a more simplified method. Unlabeled data batch  $\mathcal{U} = \{u_b, b \in (1, \dots, \mu B)\}$  is now  $\mu$ -times bigger. Given the model's prediction  $q_b$  for a weakly augmented unlabelled sample  $u_b$ , method yields hard pseudo-labels  $\hat{q}_b = \text{argmax}(q_b)$  and  $\hat{\mathcal{U}} = \{(u_b, q_b, \hat{q}_b)\}$ . Afterwards, the model predicts labels for both a batch of weakly augmented labelled images and a batch of strongly augmented unlabelled images. Only the confident predictions for unlabelled samples are used in the

final unsupervised part of the loss. They are filtered with the threshold  $\tau$ . The loss of FixMatch is then the sum of two categorical cross-entropies for labelled and unlabelled images:

$$\mathcal{L} = \frac{1}{B} \sum_{(x,y) \in \mathcal{X}} H(y, f_M(\alpha(x); \theta)) + \frac{\lambda_u}{\mu B} \sum_{(u,q,\hat{q}) \in \hat{\mathcal{U}}} \mathbb{1}_{\max(q) > \tau} H(\hat{q}, f_M(\mathcal{A}(u); \theta)) \quad (2)$$

As we use  $\tau$  for filtering confident pseudo-labels, we do not need the linear ramp-up for  $\lambda_u$ .

## B. Experiments

### B.1. Transfer learning

We took a version of Wide ResNet-50-2 pre-trained on ImageNet from PyTorch.<sup>2</sup> Transfer learning was fine-tuned for every individual  $n_l$ , as it did not require much computational budget:

- learning rate  $\in \{1 * 10^{-3}, 5 * 10^{-4}\}$
- optimizer weight decay  $\in \{0.0, 0.0001\}$
- layers freezing  $\in \{\text{Fine-tuning, Feature extraction}\}$  (see Section 3.1)

Further hyperparameters are kept fixed, namely we use Adam optimizer [33],  $B = 32$ , number of epochs = 50. Additionally, early stopping with the patience of 25 epochs was applied to avoid overfitting.

### B.2. MixMatch & FixMatch

Hyperparameter fine-tuning for both SSL methods was two-fold: firstly, we fine-tuned more general parameters on 200 labelled samples ( $n_l = 200$ ) with respect to the validation loss (see Table 4). Secondly, for each specific  $n_l$ , we tuned subset-size-dependent parameters.

The labeled batch size was  $B = 16$  for both algorithms. Additionally, we fix  $\mu = 4$ ,  $\tau = 0.7$  for FixMatch. We omit using cosine learning rate decay.

Regarding secondary fine-tuning, after the increase of  $n_l$ , each epoch becomes proportionally longer. Thus, we propose the following inverse formula to define the number of epochs:

$$\text{Number of epochs} = \text{round} \left( \frac{n_B}{n_l \text{ div } B} \right), \quad (3)$$

<sup>2</sup>[https://pytorch.org/hub/pytorch\\_vision\\_wide\\_resnet/](https://pytorch.org/hub/pytorch_vision_wide_resnet/).



Hyperparameter	MixMatch	FixMatch
Learning rate	{ <b>0.01</b> , 0.001}	{ <b>0.03</b> }
Optimizer	{ <b>Adam</b> }	{Adam, <b>SGD</b> }
Number of epochs	{500, <b>1000</b> }	{1000, <b>2000</b> }
$T$	{0.25, <b>0.5</b> , 0.75, 0.9}	—
$\alpha$	{0.25, 0.5, 0.75, <b>0.9</b> }	—
$\lambda_u$	{12.5, 25, 50, 100, 150}	{ <b>5.0</b> , 25.0}
Grid-search size	320	8

**Table 4.**

Primary hyperparameter search grid for SSL methods. Best value is marked with bold font. SGD – stochastic gradient descent with momentum ( $\beta = 0.9$ ) [34]. An epoch is defined by maximum number of batches in labelled subset.

where  $n_B$  denotes total number of labelled batches, used while training.

While secondary fine-tuning, we vary:

- $\beta_{\text{EMA}} \in \{0.0, 0.999\}$  (EMA decay)
- $n_B \in \{12000, 15000\}$  for MixMatch /  
 $n_B \in \{24000, 30000\}$  for FixMatch